SLOVAK UNIVERSITY OF TECHNOLOGY IN BRATISLAVA

Faculty of Electrical Engineering and Information Technology

Reg. No.: FEI-104400-74052

Ing. Martin Kucharovič

Dissertation Thesis Abstract

Optimizing the shielding capabilities of the magnetic cloak

Submitted to obtain the academic title of

"philosophiae doctor", abbreviated as "PhD."

In the doctorate degree study programme:	Physical Engineering
In the field of study:	Electrical and Electronics Engineering
Form of Study:	full-time

Bratislava, June 24, 2024

Dissertation Thesis has been prepared at

Institute of Electrical Engineering SAS

Submitter: Ing. Martin Kucharovič

Institute of Electrical Engineering SAS

Dúbravská cesta 9, 841 04, Bratislava

Supervisor: Mgr. Mykola Soloviov, PhD.

Institute of Electrical Engineering SAS

Dúbravská cesta 9, 841 04, Bratislava

Readers: prof. Ing. Vladimír Jančárik, PhD.

Faculty of Electrical Engineering and Information Technology of STU in Bratislava

Ilkovičova 3, 841 04, Bratislava

RNDr. Gabriel Pristáš, PhD.

Institute of Experimental Physics,Slovak Academy of Sciences

Watsonova 47, 040 01, Košice

Dissertation Thesis Abstract was sent _____

Dissertation Thesis Defence will be held on _____ *at*_____ *(am/pm)*

at Institute of Electrical Engineering SAS, Dúbravská cesta 9, 841 04 Bratislava

prof. Ing. Vladimír Kutiš, PhD.

Dean of FEI STU

_____

Abstrakt

Táto dizertačná práca sa zaoberá problematikou zlepšenia tienenia magnetického poľa Zeme v magnetickom plášti. V našom prípade sú na supravodivú časť plášťa použité CC HTS pásky. Počas ochladzovania plášťa obsahujúceho takúto supravodivú vrstvu v zemskom magnetickom poli dochádza k tomu, že toto pole zostane zachytené v plášti. Plášť teda po ochladení tieni magnetické polia, avšak v jeho objeme nie je magnetické pole nulové. Štúdia skúma dynamický magnetorezistentný efekt na zníženie zvyškového magnetického poľa aplikáciou axiálneho striedavého magnetického poľa, čo zahŕňa striedavé obdobia demagnetizácie a relaxácie.

Na tento účel bola vytvorená aparatúra umožňujúca dosiahnutie takéhoto demagnetizačného efektu. Výsledky demagnetizačných meraní ukázali, že naším postupom je možné znížiť zachytené magnetické pole. Avšak počas týchto experimentov bol zistený problém, že od istého bodu výsledky neboli stabilne reprodukovateľné. Preto sa súčasne s demagnetizačnými meraniami merala aj susceptibilita, nakoľko boli dostupné referenčné dáta plášťov a bolo možné ich porovnať, či sa nejakým spôsobom nemenia ich vlastnosti.

Zistilo sa, že v plášťoch došlo k zmene ich účinnosti tienenia, a preto sa začalo skúmanie príčiny tohto javu. V rámci skúmania degradácie boli realizované transportné merania, magnetické mapovanie, SEM a EDX analýzy na samotných páskach po rozobratí plášťa. Štúdia identifikuje potenciálne faktory, ktoré mohli spôsobiť alebo prispieť k degradácii HTS pások. Najpravdepodobnejším variantom je, že poškodenie striebornej krycej vrstvy CC pásky naštartovalo proces dekompozície REBCO vrstvy na nesupravodivú fázu. Externé sily, ktoré poškodili striebornú vrstvu, mohli poškodiť aj samotnú REBCO vrstvu, čo ukazujú mapovacie merania. Zníženie výkonu pásky sa teda javí ako kombinácia viacerých faktorov.

Výskum ukazuje, že odstránenie magnetického poľa z objemu magnetických plášťov je možné pomocou dynamickej magnetorezistencie. Zároveň však podčiarkuje potrebu lepšieho porozumenia procesom degradácie s cieľom zvýšiť dlhodobú stabilitu a účinnosť HTS materiálov v aplikáciách magnetického tienenia.

Abstract

This dissertation addresses the issue of improving the shielding of the Earth's magnetic field in the magnetic cloak. In our case, CC HTS tapes are used for the superconducting part of the cloak.During the cooling of the cloak containing such a superconducting layer in the Earth's magnetic field, this field remains trapped in the cloak. Therefore, after cooling, the cloak shields magnetic fields, but the magnetic field within its volume is not zero. The study investigates the dynamic magnetoresistance effect to reduce the residual magnetic field by applying an axial alternating magnetic field, which involves alternating periods of demagnetization and relaxation.

For this purpose, an apparatus was developed to achieve such a demagnetization effect. The results of the demagnetization measurements showed that our method can reduce the trapped magnetic field. However, during these experiments, a problem was identified where the results were not consistently reproducible after a certain point. Therefore, in parallel with the demagnetization measurements, susceptibility was measured since reference data on the cloaks were available, allowing for comparison to determine if their properties had changed in any way.

It was found that the cloaks' shielding effectiveness had changed, prompting an investigation into the cause of this phenomenon. As part of the degradation investigation, transport measurements, magnetic mapping, and SEM and EDX analyses were carried out on the tapes themselves after disassembling the cloak. The study identifies potential factors that could have caused or contributed to the degradation of the HTS tapes. The most likely scenario is that damage to the silver coating layer of the CC tape initiated the decomposition process of the REBCO layer into a non-superconducting phase. External forces that damaged the silver layer could have also damaged the REBCO layer itself, as indicated by the mapping measurements. Therefore, the reduction in tape performance appears to be a combination of several factors.

The research shows that it is possible to remove the magnetic field from the volume of magnetic cloaks using dynamic magnetoresistance. However, it also underscores the need

for a better understanding of degradation processes to increase the long-term stability and effectiveness of HTS materials in magnetic shielding applications.

Contents

Bibliography

Introduction

The field of superconductivity has long promised revolutionary advancements in numerous applications, from powerful electromagnets for MRI devices and fusion reactors to lossless energy transmission through superconducting cables. At the core of these applications are high-temperature superconductors (HTS) and their ability to maintain zero electrical resistance and expel magnetic fields (Meissner effect) at relatively higher temperatures compared to previously used low-temperature superconductors (LTS). For effective utilization of these properties in practical applications, such as magnetic shielding, the durability and performance of superconducting conductors are paramount; therefore, REBCO (Rare Earth Barium Copper Oxide) CC (Coated Conductor) tapes are used for these applications.

Magnetic shielding is a crucial aspect of many technological applications. The study of magnetic field shielding using superconducting and ferromagnetic materials has garnered significant attention due to its potential applications in various fields such as medical imaging, particle accelerators, and electronic devices. The ability to effectively shield magnetic fields is critical for enhancing the performance and lifespan of sensitive devices and ensuring measurement accuracy. Instead of high-permeability materials used in conventional applications, superconducting materials can also be used for this purpose. However, high-temperature superconducting materials cannot completely shield the magnetic field unless they are brought to the superconducting state in a field-free environment.

The main issue encountered with this cloak is that when cooling the superconductor in the Earth's magnetic field, this field remains trapped within the volume of the magnetic cloak.

There are several possible solutions to this problem, but two realistic approaches were identified. The first option is to transition the superconductor to the superconducting state in a shielded chamber where no magnetic field is present. The second option is to expel the magnetic field from the volume of the cloak after it has been cooled.

This research focuses on the application of the physical phenomenon of dynamic magnetoresistance combined with the rotation of the magnetic cloak. Using dynamic magnetoresis-

tance, we change the magnitude and arrangement of persistent currents in the superconductor through a transverse alternating magnetic field. This approach aims to achieve an ideal value as close to 0 T as possible.

During this research, it was found that the superconducting tapes used in the magnetic cloak degraded over time. Although examining this degradation was not the original motivation, it became a significant issue due to its impact on the performance and lifespan of magnetic cloaks. Therefore, part of this work also focuses on examining the extent and causes of HTS tape degradation. This secondary objective aims to improve the understanding of material behavior under operational conditions and develop strategies to mitigate such degradation, thereby increasing the long-term reliability and durability of magnetic shielding.

1. Magnetic Cloak

The concept of a magnetic cloak involves creating a device capable of shielding or masking the internal space from external magnetic fields, ensuring that no magnetic field affects the object inside. Additionally, the ambient magnetic field around the superconducting cloak remains unchanged and undistorted, thereby preserving the integrity of the external field. Thus, a superconducting cloak should fulfill two conditions:[1, 2, 3]

1. Zero magnetic field inside the superconducting cylinder in the magnetic cloak.

2. The unaltered ambient magnetic field of the magnetic cloak.

A magnetic cloak operates on the principle of combining superconducting (SC) and ferromagnetic (FM) parts in a coaxial arrangement. [1, 2, 3] The inner part is made of a superconducting material, which exhibits perfect diamagnetism and expels magnetic flux from its volume. [2, 4] The outer part of the cloak is made of ferromagnetic material, which has constant permeability and attracts magnetic flux into its volume. This arrangement ensures that the inner tube shields against the penetration of the magnetic field, providing effective magnetic shielding for any object placed inside. The result of shielding is not dependent on the intensity of the applied magnetic field.[2, 4]

1.1 Ferromagnetic Cylinder

For the ideal functionality of the magnetic cloak, a precise balance of magnetic moments created by individual parts of the cloak is required. Therefore, the ferromagnetic part of the cloak must meet the condition for relative magnetic permeability:[1, 3, 5]

$$\mu_r = \frac{R_2^2 + R_1^2}{R_2^2 - R_1^2} \tag{1.1}$$

where μ_r is the relative permeability, R_1 is the inner radius of the ferromagnetic cylinder, and R_2 is the outer radius of the ferromagnetic cylinder.

1.2 Superconducting Cylinder

The superconducting part of the cloak utilizes commercially available REBCO superconductors in the form of coated conductors. These conductors are strips with various internal configurations, advantageous for their lower costs, improved mechanical properties, flexible dimensions, and competitive critical current density (J_c) values. High-temperature superconductors like REBCO operate at critical temperatures above 90 K. However, HTS materials are Type-II superconductors, meaning they can trap magnetic flux within their volume in a magnetic field.

For the cloak, tapes from Superpower (SF12050AP) and Fujikura (FYSC-SCH12) were used. The superconducting parts were wound helically or aligned longitudinally, with adhesive securing the CC tapes to the glass laminated cylinder.

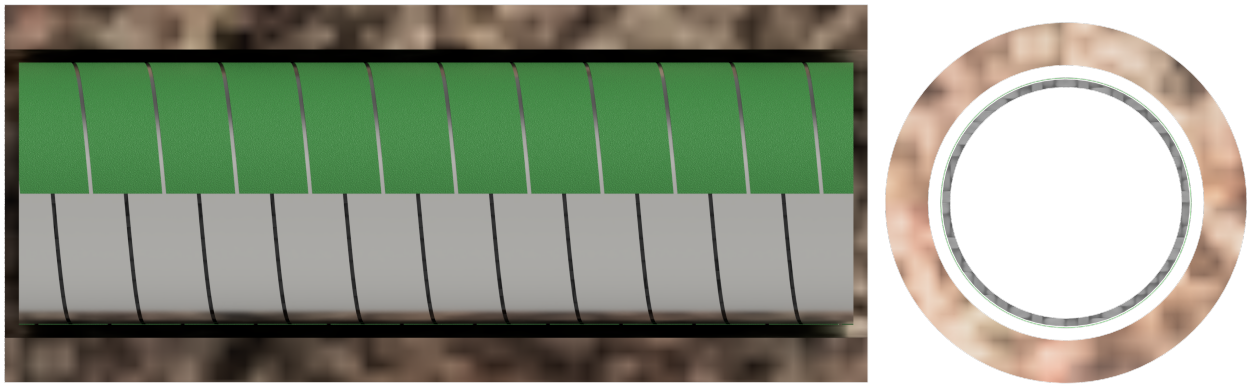

(a) *Cross section of the ferromagnetic cylinder* **(b)** *Top view of the cloak*

Figure 1.1: *A rendered image of the magnetic cloak*

2. Methodology and Results of the Transverse Field Demagnetization

When the magnetic cloak is cooled in an external field, this field remains trapped in the cloak. The work explores the development and implementation of a magnetic cloak that can expel the trapped magnetic field within its volume by utilizing the dynamic magneto-resistance effect. The goal is to reduce the internal magnetic field to nearly zero, with an optimal target range of a few microteslas (μT), representing an 85-95% decrease compared to the Earth's magnetic field. This reduction is achieved through a carefully designed experimental setup.

2.1 Measurement of Demagnetization

The experimental apparatus consists of several key components and devices that are shown in Fig.2.1.

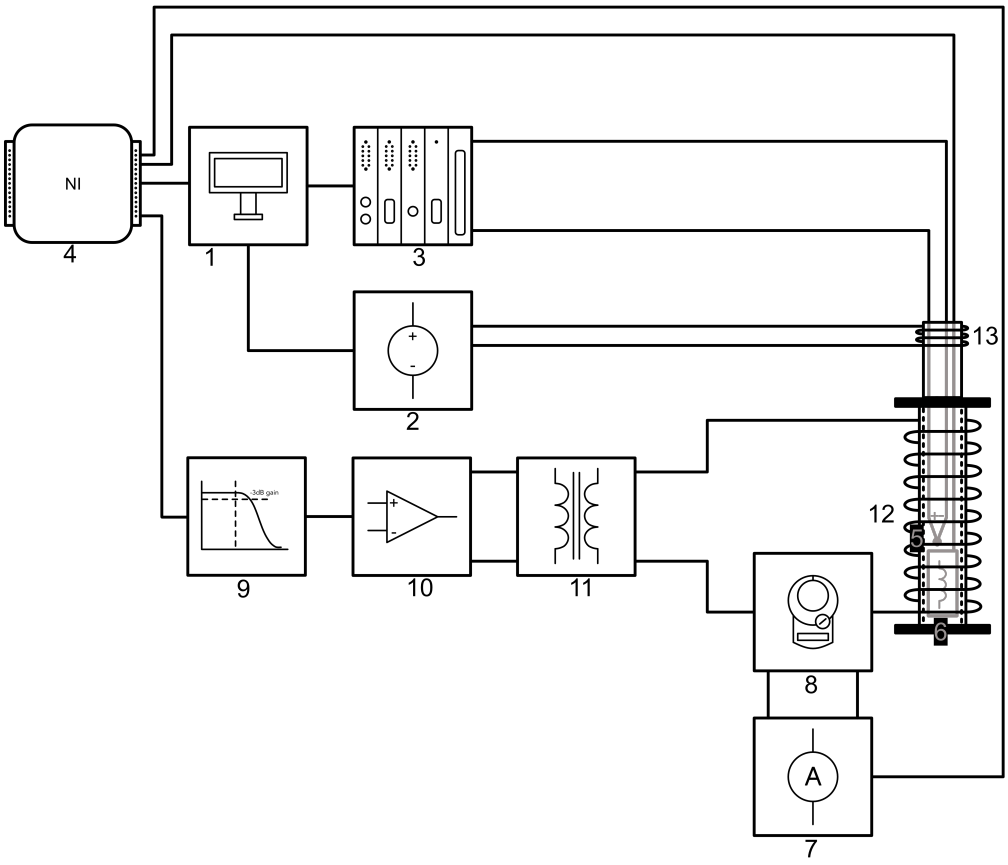

Figure 2.1: *Wiring diagram: 1. Computer, 2. DC power supply (Aimtti - CPX400DP), 3. Plug-in measuring module (Dewetron - PAD-TH8-P 8-channel A/D converter and RTD), 4. Measuring card (National Instruments - USB-6001), 5. Thermocouple (Type T - Copper/Constantan), 6. Magnetic field sensor (Stefan Mayer - FLC3-70), 7. Measuring instrument (HIOKI - CM7291), 8. Clamp probe, 9. RC filter, 10. Audio amplifier (QSC - RMX 5050), 11. Transformer, 12. Magnetization coil, 13. Resistive bifilar winding.*

These components are configured in a complex wiring diagram that includes circuits for field measurement, generating of the demagnetization field, and temperature stabilization. LabVIEW software is employed for two main purposes: the demagnetization process which includes trapped field measurement and signal generation, and maintaining a constant temperature at the magnetometric sensor. The LabView application is also used for rough data processing from the DAQ card as well as for demagnetizing waveform generation using the DA converter on the same card.

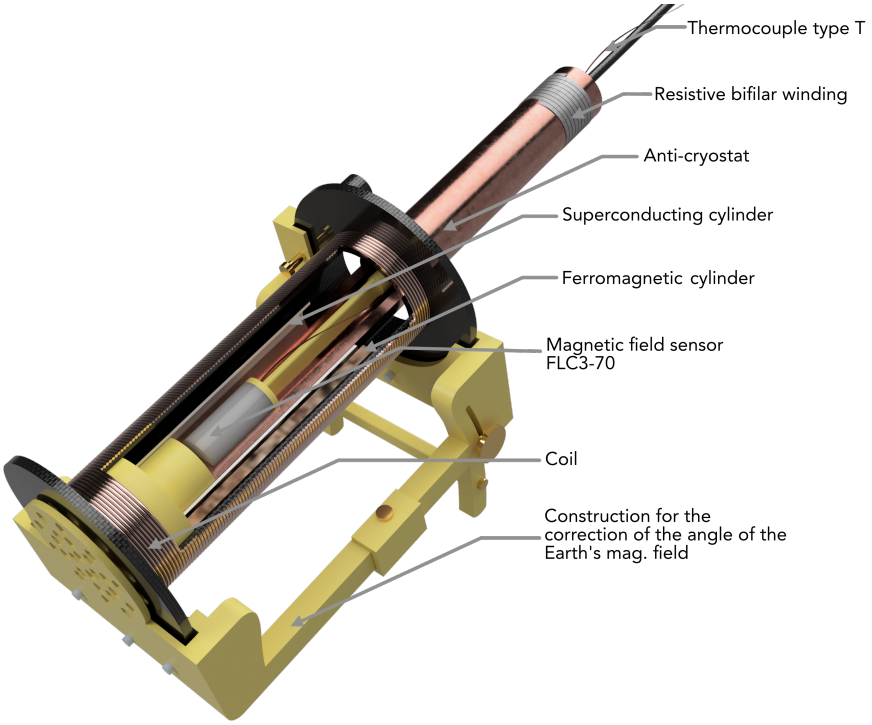

Figure 2.2: *Detailed model of the experimental system.*

Before demagnetization, necessary measurement parameters are set in the software and instruments.

These are the steps in the demagnetization process:[6]

1. Initial placement ensures that the Earth's magnetic field is perpendicular to the central axis of the cloak.

2. The setup is filled with liquid nitrogen (LN_2), and the anti-cryostat's heating is activated.

3. When the system has cooled down the entire system is rotated 180° against Earth's magnetic field, placing the trapped field and Earth's field in an antiparallel configuration.

4. Demagnetization process which is conducted in two stages

    - Demagnetization phase - The actual process of generating the demagnetization field where the amplitude increases with each iteration.

- Relaxation phase - Ensures the stabilization of measured values before recording the magnetic field within the cloak.

Field Measurement Circuit

The field measurement circuit (Fig.2.3) utilizes a magnetic field sensor connected to a DAQ card. The sensor measures the magnetic dipole moment through inductive sensing coils, and the DAQ card processes the signals. The software developed in LabVIEW processes the raw data to determine the magnitude and orientation of the magnetic field.

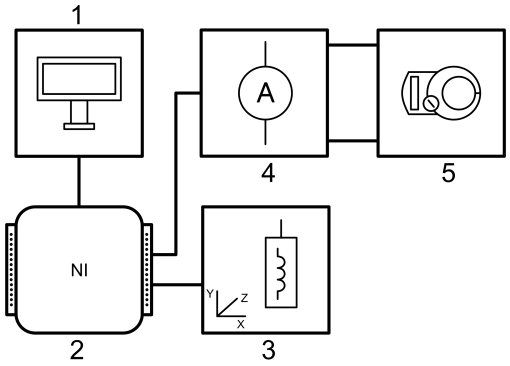

Figure 2.3: *Wiring diagram of the field measurement circuit: 1. Computer, 2. Measuring card (National Instruments - USB-6001), 3. Magnetic field sensor (Stefan Mayer - FLC3-70), 4. Measuring instrument (HIOKI - CM7291), 5. Clamp probe.*

Axial Demagnetization Field Circuit

The demagnetization field circuit (Fig.2.4) includes a DAQ card, RC filter, amplifier, transformer, and coil. A sinusoidal signal is generated and smoothed by the RC filter before being amplified to create the demagnetization field. The current in the coil is monitored using a clamp ammeter, and the generated magnetic field is calculated using an empirical equation.

$$B_d = 0.848 \cdot I_{coil} \tag{2.1}$$

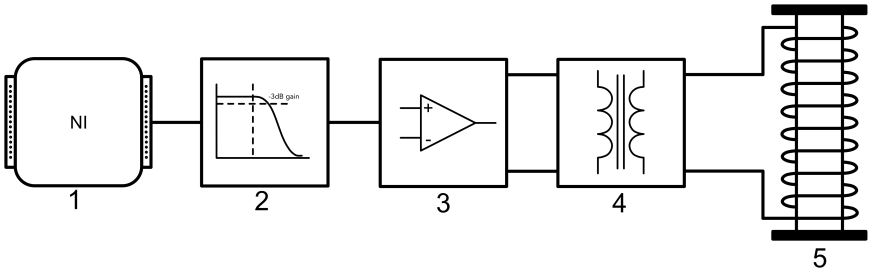

Figure 2.4: *Wiring diagram of the axial demagnetization field circuit: 1. Measuring card (National Instruments - USB-6001), 2. RC filter, 3. Audio amplifier (QSC - RMX 5050), 4. Transformer, 5. Magnetization coil.*

Temperature Stabilization Circuit

The temperature stabilization circuit (Fig.2.5) consists of a bifilar heating winding, anti-cryostat, thermocouple, modular plug-in system, and DC power source. The PID control system in LabVIEW ensures precise temperature settings, crucial for maintaining stable conditions during measurements. The anti-cryostat is designed to mitigate the temperature transition from liquid nitrogen to the magnetic sensor, using both passive insulation and active heating elements.

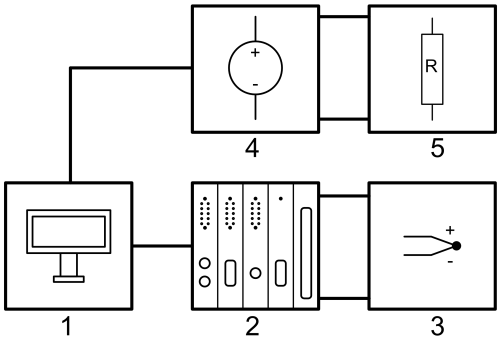

Figure 2.5: *Wiring diagram of the temperature stabilization circuit: 1. Computer, 2. Plug-in measuring module (Dewetron - PAD-TH8-P 8-channel A/D con- verter and RTD), 3. Thermocouple (Type T - Copper/Constantan), 4. DC power supply (Aimtti - CPX400DP), 5. Bifilar resistive winding.*

2.2 Results and Discussion

Using MATLAB for data analysis, a comprehensive evaluation of experimental data was conducted. This included applying mathematical and statistical methods, enabling a thorough exploration of data properties and trends.

Helical Geometry Results

SuperPower Tape

Initial measurements provided insights for improving procedures. Notably, a residual magnetic field value of $B_{Rem} = 0.142$ µT was achieved from the initial value of $40.22\mu T$, indicating a reduction by a factor of 280 compared to the external magnetic field.

Statistical evaluation of 21 measurements revealed an average magnetic field reduction in the cloak by approximately a factor of 23.25 from its initial value. That means the average value of the captured magnetic field in the cloak was 1.7816 µT, while the initial average value of the frozen field in the cloak was 41.4207 µT. Expressed in percentages, this means an average reduction of 95.70% and a peak reduction of 99.66%.

The range of the lowest measured magnetic field values varied from 1.669 to 4.22 µT.

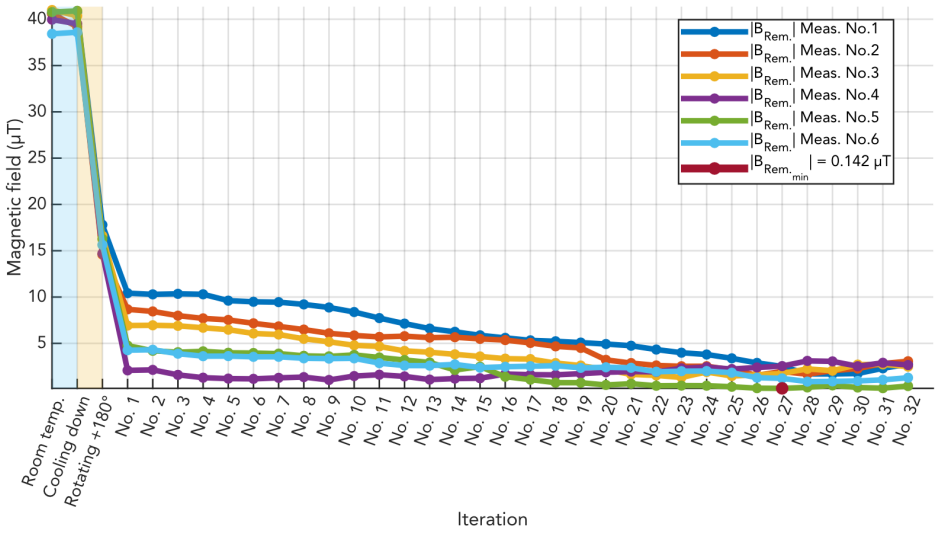

Figure 2.6: *Demagnetization Graph - Multiple Measurements*

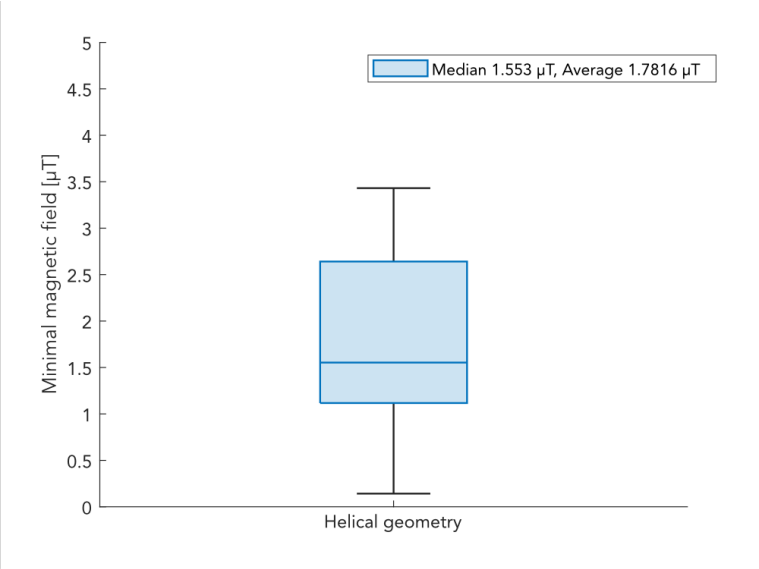

Figure 2.7: *Box Graph of Magnetic Fields After Demagnetization*

Fujikura Tape

Results were less effective, with a lowest recorded magnetic field value of $B_{Rem} = 37.814$ µT, indicating a reduction by a factor of 1.1. This tape has a much higher critical current and a slightly different structure. The existing setup is not able to generate a magnetic field high enough to effectively demagnetise this tape.

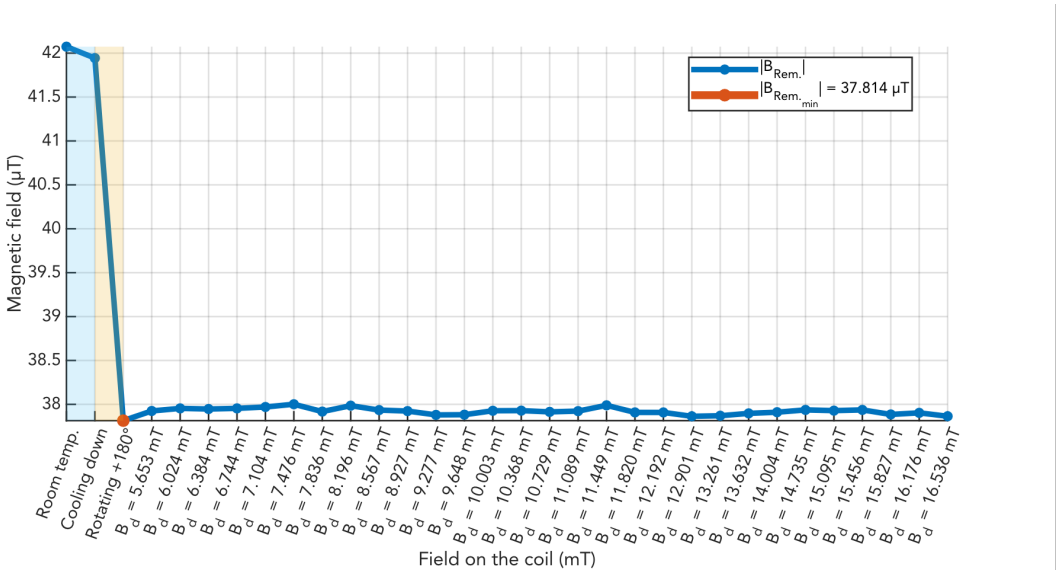

Figure 2.8: *Demagnetization graph - Best measurement*

Longitudinal Geometry Results

SuperPower Tape

The lowest achieved magnetic field in this geometry was $B_{Rem} = 1.699\mu T$ from the initial external magnetic field value of 37.735 µT. This indicates a reduction of the external magnetic field by a factor of 22. The average value of the trapped magnetic field in the cloak is $B_{Rem} = 3.0839\mu T$, with the initial average value of the frozen field in the cloak being 37.575 µT. This represents an average reduction of the magnetic field in the cloak by a factor of 12.18 compared to its initial value. In percentages, this means an average reduction of 91.79% and a peak reduction of 95.48%.

The range of the lowest measured magnetic field values varied from 1.669 to 4.22 µT. This result suggests that the demagnetization efficiency in this geometry was lower than in the previous case.

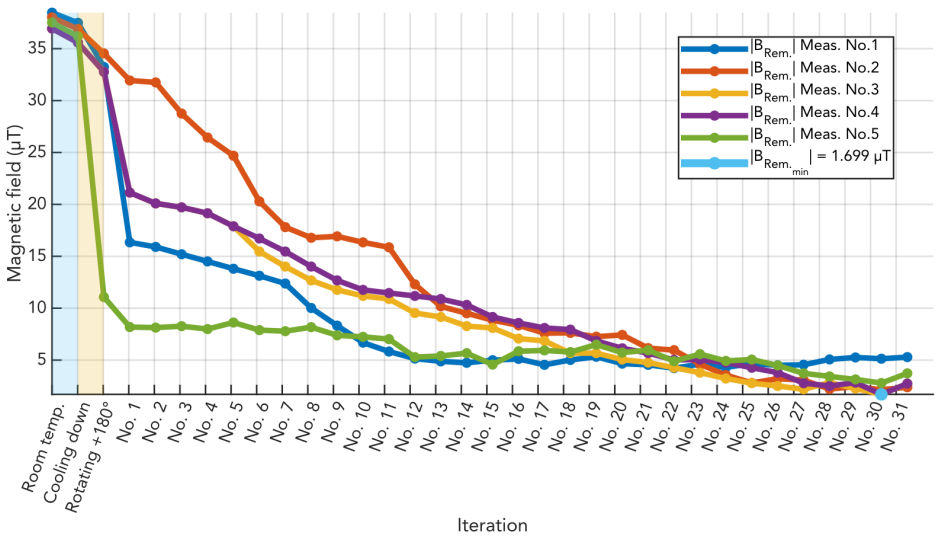

Figure 2.9: *Demagnetization graph - Multiple measurements*

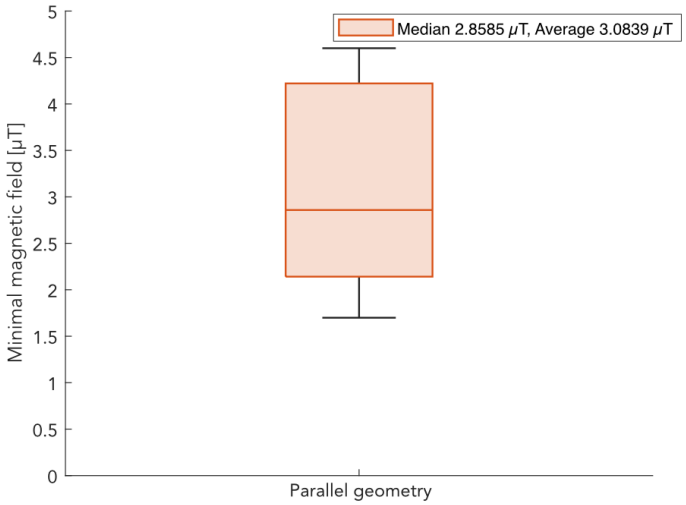

Figure 2.10: *Box Graph of Magnetic Fields After Demagnetization*

The comparison showed better results for helical geometry than longitudinal geometry, partly due to rapid degradation in longitudinal geometry, limiting optimization.

Degradation of the superconducting tape was observed, affecting the shield's performance. The normalized magnetic field change after rotation by 180° indicated loss of shielding capability. This phenomenon was more pronounced in longitudinal geometry, with helical geometry likely degrading earlier.

3. Methodology and Results of the Investigation of Defects of CC Tapes

3.1 Non-Destructive Measurement

3.1.1 Susceptibility Measurement

In this case, complex susceptibility, which has two components, is measured. The real part (χ') represents the slope of the hysteresis curve or the shielding efficiency of the magnetic cloak. For ferromagnetic materials, χ' is a positive value, while for superconducting materials it is typically negative. An ideal magnetic cloak that combines these two materials would have a χ' close to zero.[7]
The imaginary part (χ'') represents energy absorption and can only have positive values. There is only one way to reduce this part, which is to minimize AC losses in both components of the magnetic cloak.[1, 5, 7, 8]

3.1.1.1 Measurement of Susceptibility

Racetrack coils were used for this measurement, which was connected as a "Calibration-free system".[2, 5, 7] This means we have a system of two coils, one measuring and the other compensating to equalize the inductances and eliminate unwanted signals, which ensures that the measured signal comes only from the sample and not from the coils or other system components.

The measurement apparatus consists of several components. Fig.3.1 shows the wiring diagram along with the instruments used for the measurement.

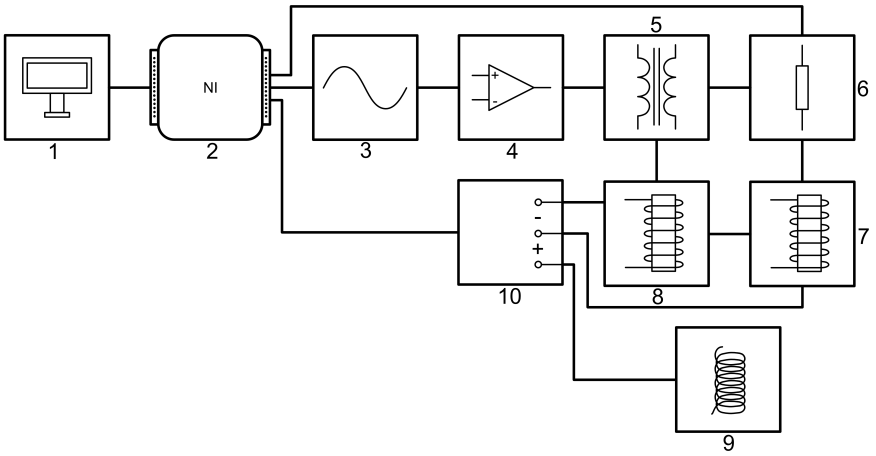

Figure 3.1: *Wiring diagram of the susceptibility measurement: 1. Computer, 2. Measurement Card (National Instruments - USB-6211), 3. Signal Generator (Tabor - arbitrary waveform generator 8025), 4. Audio Amplifier (QSC - RMX 5050), 5. Transformer, 6. Non-inductive Shunt resistor, 7-8. Pair of Solenoid Measurement Coils, 9. Small Multi-Turn Coil, 10. Summation/Compensation Box*

3.1.1.2 Results and Discussion

Data analysis using MATLAB software involved recalculating the measured data using the provided equations. The results are compared with reference data from the time of production to assess degradation.

Helical Geometry

SuperPower Tape

Initial measurements showed good shielding capability, but significant degradation of this capability was observed over time. As previously mentioned, an ideal shield should have its hysteresis curve lie at zero value and have the smallest possible area. In this context, the slope of the hysteresis curve can be understood as the shielding effect of the magnetic shield, and the area of the curve as its energy losses. The closest value to this described ideal is the reference value with six layers. The curves representing the current measurements show a significant degradation. The difference between the best and worst value is approximately $0.8\ A \cdot m^2$.

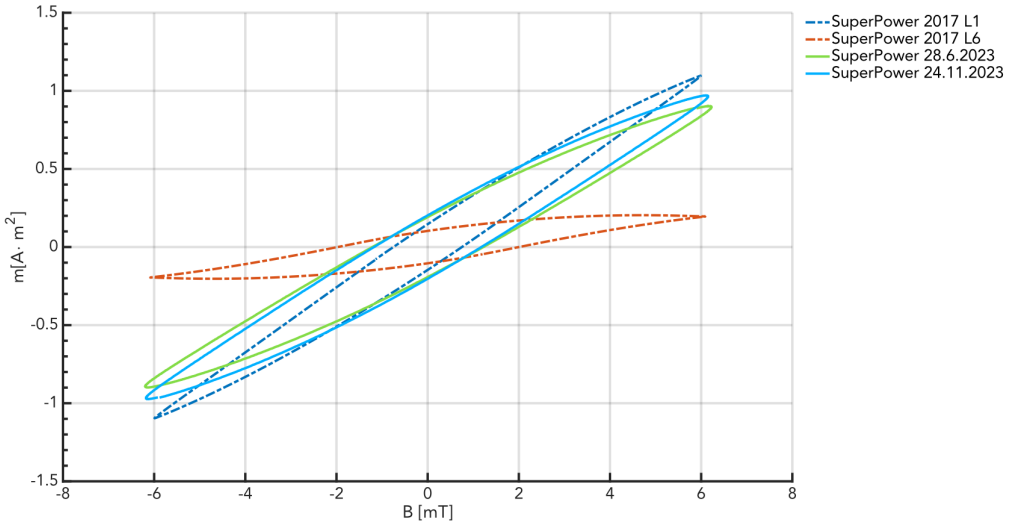

Figure 3.2: *Hysteresis loops Cloak*

Fujikura Tape

Measurements were conducted in a limited range due to difficulties in expelling the magnetic field. With this tape, we also observe some shifts in the properties of this superconducting part, but the changes are much smaller than with the SuperPower tape. In this case, the difference between the best and worst value is approximately 0.03 $A \cdot m^2$.

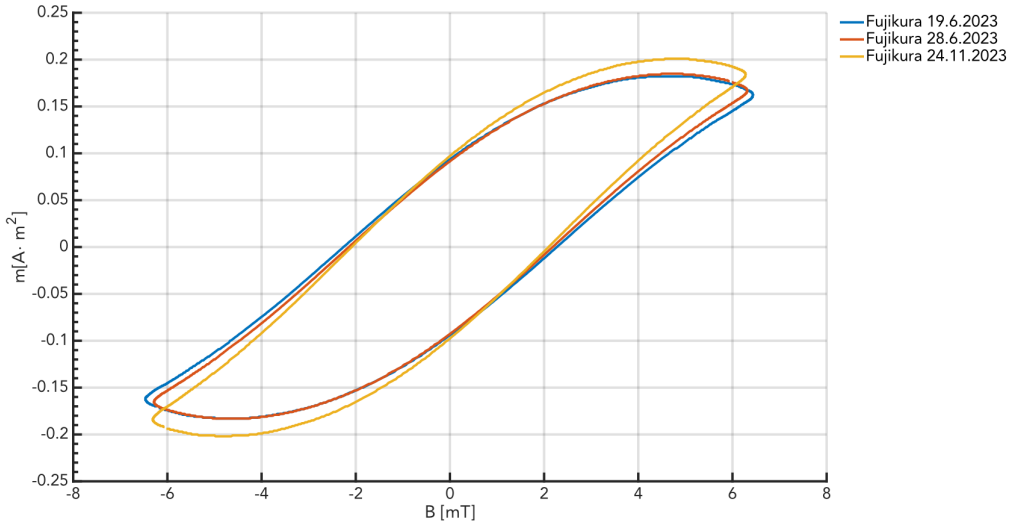

Figure 3.3: *Hysteresis loops Cloak*

Longitudinal Geometry

SuperPower Tape

Similarly to the helical geometry, the same effect was observed with increased energy losses and reduced shielding effects. Essentially, we can conclude that both geometries with SuperPower tape experienced the same extent of property degradation. In this case, the difference between the best and worst value is approximately 0.7 $A \cdot m^2$.

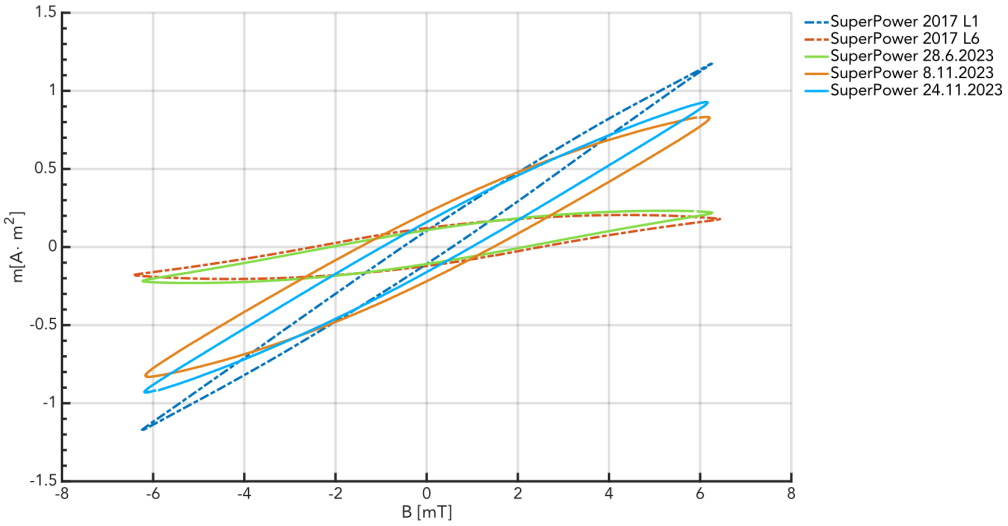

Figure 3.4: *Hysteresis loops Cloak*

3.2 Destructive Measurement

After discovering significant degradation in the superconducting tapes used in the magnetic cloak, a detailed investigation was initiated to assess the extent of the damage. This work focuses on one specific superconducting cylinder using three main experiments:

1. Transport measurement of critical current.
2. Magnetic field mapping over the sample surface.
3. Scanning electron microscopy (SEM) and dispersive spectroscopy (EDX).

These experiments aim to provide a comprehensive understanding of the damage.
The cloak with longitudinal geometry was selected due to the pre-cut tapes, which save time

and allow precise identification of tape origin and damage extent. The tapes are slightly longer than necessary for transport measurements, allowing for thorough examination of approximately 5-9 cm of each tape.

3.2.1 Transport Measurement of Critical Current

The wiring diagram of this measurement is shown in the Fig.3.5. Equipment called "multi-tap" is used to measure transport currents and consists of 23 pressure voltage contacts that allow measurement on 22 consecutive sections. The sample is fixed between current leads with pressure clamps, and voltage is measured on a reference resistor using LabVIEW software.

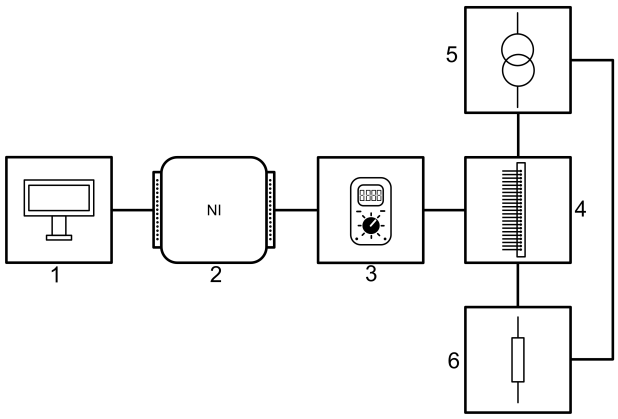

Figure 3.5: *Wiring diagram: 1. Computer, 2. Measuring card (Agilent 82357A USB/GPIB Interface), 3. Multimeter (Keithley 2700 Multimeter/Data Acquisition/Switch System), 4. Multi-tap, 5. DC power supply (Magna-Power TS Series Programmable DC Power Supply), 6. Shunt resistor* $(4 \cdot 10^{-5}\Omega)$

3.2.1.1 Results and Discussion

Critical current measurements showed significant degradation of the CC tapes. From Fig.3.6 it can be seen that the average critical current in the individual layers does not even reach the minimum value of the critical current given by the manufacturer (387 A for new tapes). The first (outer) layer showed ≈50% reduction in a critical current; the other layers $> 95\%$, indicating an almost complete loss of superconductivity. As evidenced by Fig.3.7 where it can be seen that most tapes showed a critical current up to 25 A, with only two tapes reaching a

critical current between 250 and 275 A.

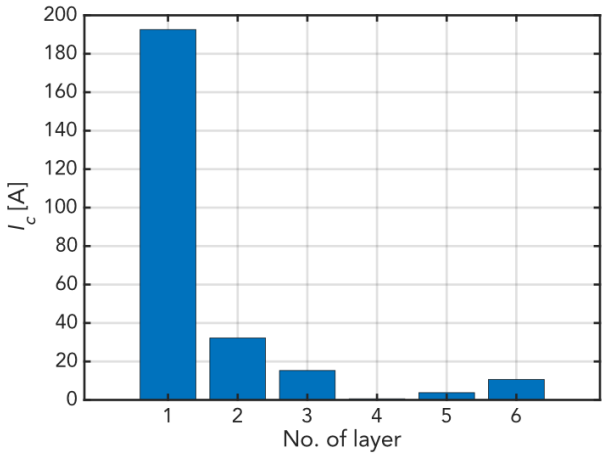

Figure 3.6: *Average critical current in individual layers*

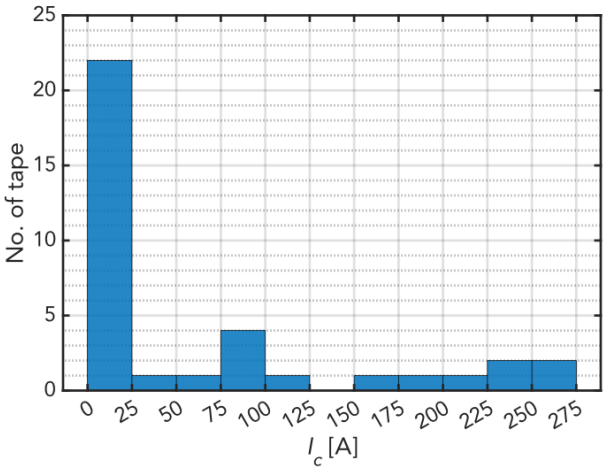

Figure 3.7: *Histogram of critical current in the superconducting part*

3.2.2 Magnetic Field Mapping

Fig.3.8 shows the wiring diagram of magnetic field mapping using a Hall probe. The Hall sensor with an active area of 50 μm x 50 μm was used to map the sample in linear, planar, and spatial modes. The mapped area was 5 cm x 2.4 cm.[10, 11]

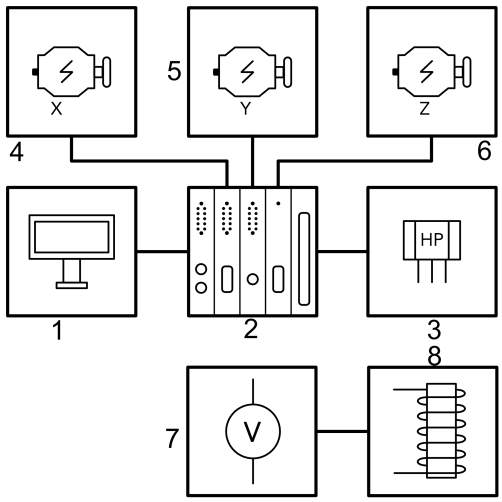

Figure 3.8: *Wiring diagram: 1. Computer, 2. Plug-in module (Dewetron - DAQP-STG Isolated strain gage amplifier and Dewetron - DAQP-V-BNC Isolated Low-Voltage Rear Plug-In Module), 3. Hall sensor, 4.,5.,6. 3-axis measuring apparatus, 7. DC power supply (Aimtti - CPX400DP), 8. Magnet*

3.2.2.1 Results and Discussion

According to Fig.3.7, three tapes were selected to include one with zero critical current (Tape No.30, $I_c = 0$ A), one with the highest critical current (Tape No.6, $I_c = 271$ A), and one with a value in between (Tape No.11, $I_c = 77$ A). Fig.3.9a shows Tape No.6, which was in the best condition, as indicated by its surface having only a few minor defects. Fig.3.9b shows Tape No.11, which had a low critical current, evident from its surface that has significant defects, including possible fractures. Fig.3.9c shows Tape No.30, which is completely degraded with no superconducting regions.

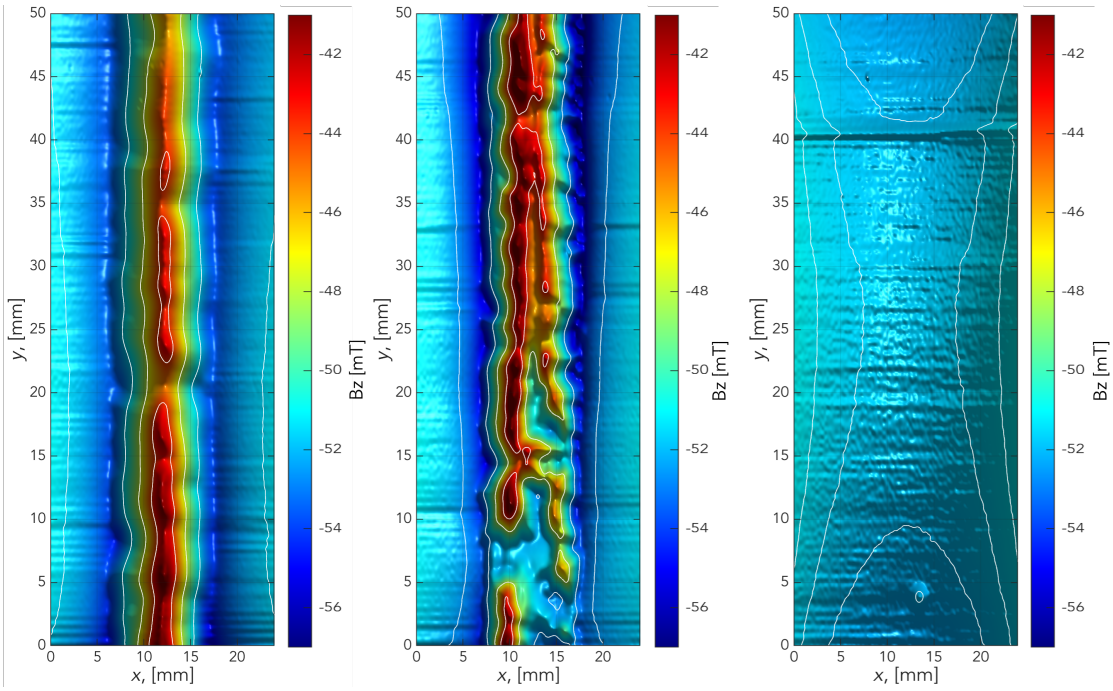

(a) *Tape No.6* **(b)** *Tape No.11* **(c)** *Tape No.30*

Figure 3.9: *z-component of magnetic flux density*

3.2.3 Scanning Electron Microscopy (SEM) and Energy Dispersive X-ray Spectroscopy (EDX)

As part of the magnetic mapping, we obtained a rough picture of what the surface of the CC tapes might look like. However, scanning electron microscopy is ideal for studying the surface structures of materials. It can reveal surface topography, the presence of cracks, defects, or other irregularities. Along with this, Energy Dispersive X-ray Spectroscopy can also be performed, which allows us to identify and quantify the chemical elements present in the sample.[12, 13, 14] Tape No.22 was selected for this measurement, which had a resistive V-A characteristic. For the REBCO layer to be visible on the tapes using this method, it was necessary to etch the silver layer.

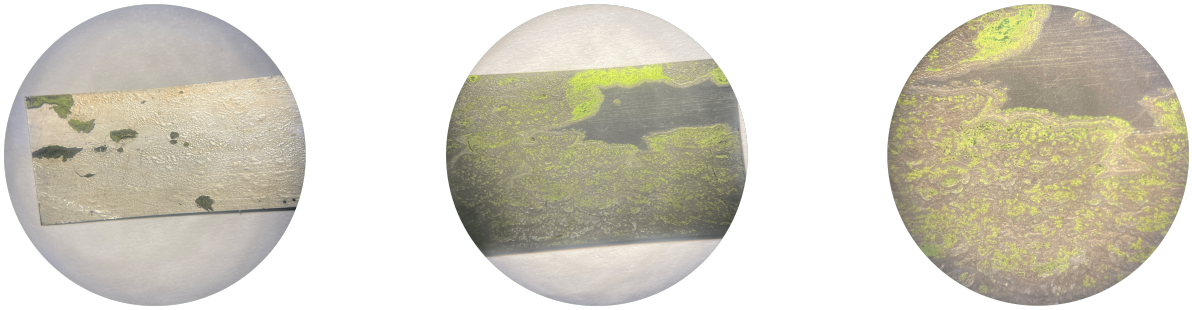

(a) *Before etching the silver layer*

(b) *After etching the silver layer*

(c) *After etching the silver layer - detail*

Figure 3.10: *Tape No.22*

3.2.3.1 Results and Discussion

Undamaged Area

Neither SEM nor EDX showed any significant REBCO structure defects in the reference region. Similarly, the chemical elements typical of REBCO superconductors had a homogeneous distribution that did not indicate any significant defects, which is shown in Fig.3.11.

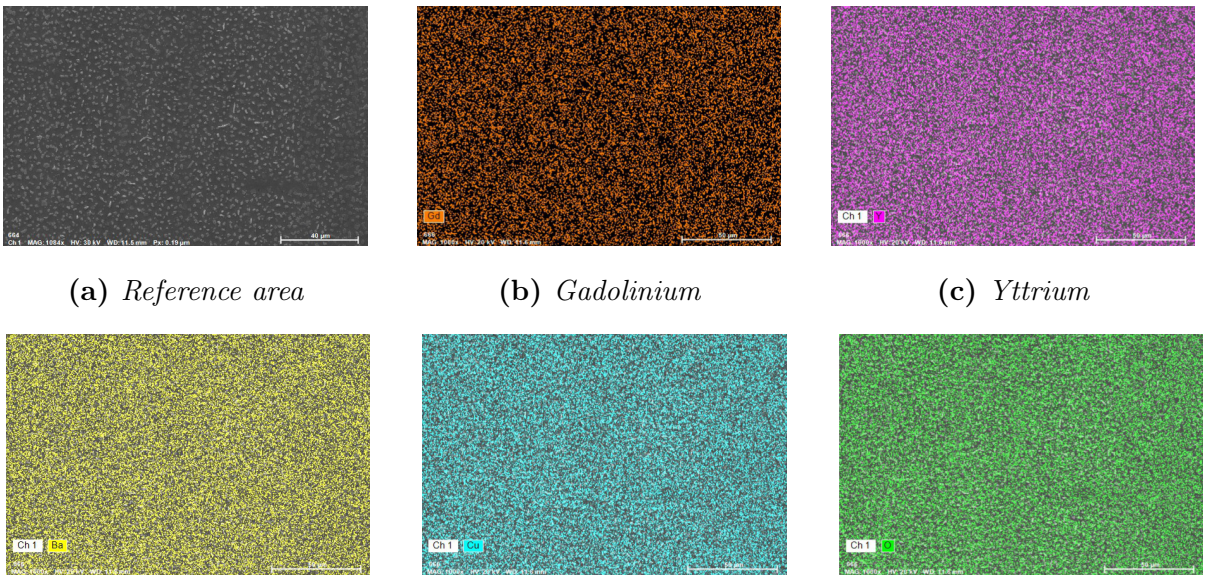

(a) *Reference area*

(b) *Gadolinium*

(c) *Yttrium*

(d) *Barium*

(e) *Copper*

(f) *Oxygen*

Figure 3.11: *Elements contained in the REBCO area*

Damaged Area

In this section, both SEM and EDX showed extensive structural damage, including delamination and a missing superconducting layer. EDX also showed changes in the chemical composition, with the presence of non-REBCO elements indicating the presence of some chemical process that may have disrupted the superconducting properties of the tapes, which is shown in Fig.3.12.

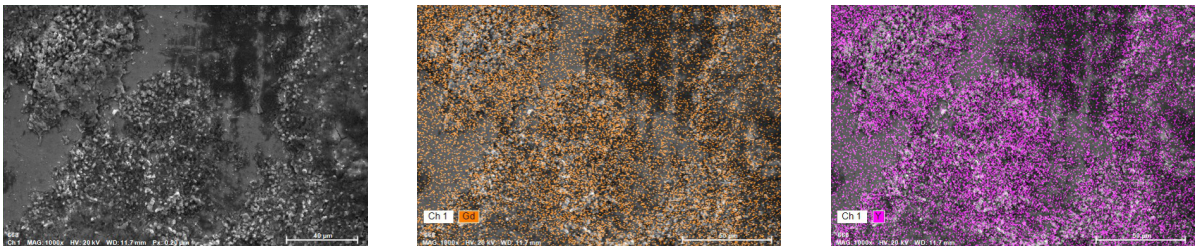

(a) *Reference area*

(b) *Gadolinium*

(c) *Yttrium*

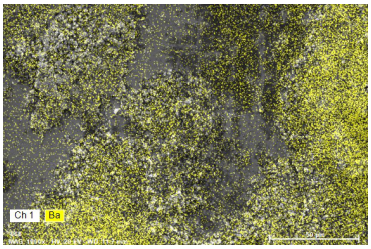

(d) *Barium*

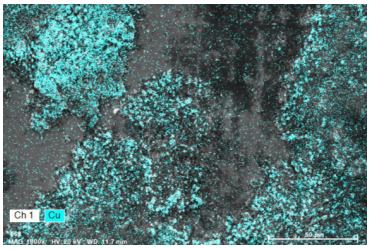

(e) *Copper*

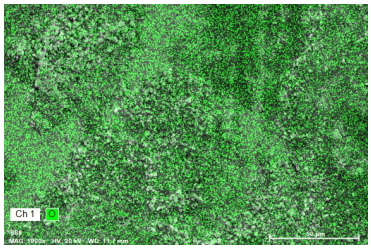

(f) *Oxygen*

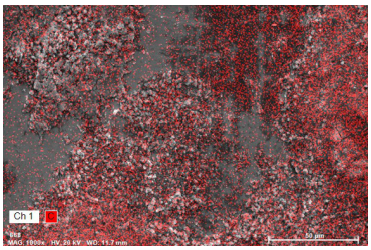

(g) *Carbon*

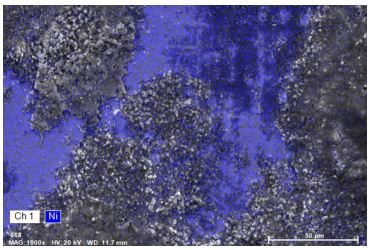

(h) *Nickel*

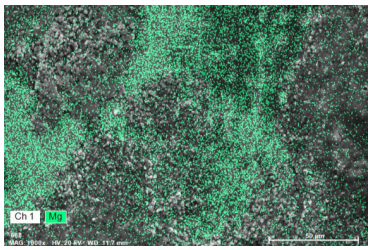

(i) *Magnesium*

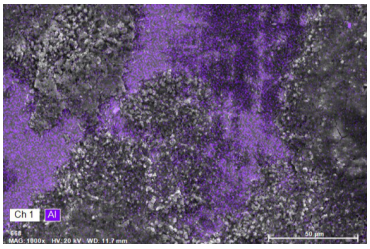

(j) *Aluminium*

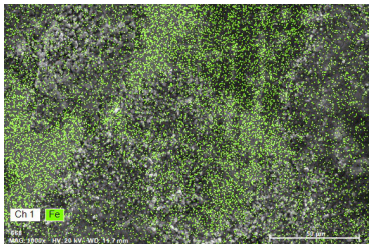

(k) *Iron*

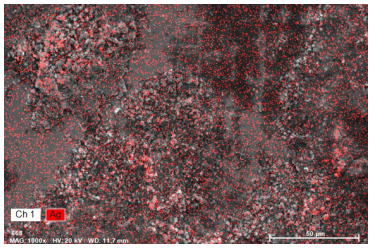

(l) *Silver*

Figure 3.12: *Elements contained in the damaged area*

The analysis of the damaged part of the superconducting tape No.22 through EDX spectroscopy revealed changes in the chemical composition compared to the undamaged part. The data indicate the presence of chemical elements that are not part of REBCO, and their non-homogeneous distribution in the damaged area suggests disruption of the integrity of the REBCO layer.

The series of Fig.3.12 shows the spatial distribution of elements in the examined area. Similar to the undamaged part, the first Fig.3.12b, 3.12c, 3.12d, 3.12e, and 3.12f focus on the chemical elements contained in the superconductor, mostly present in the REBCO layer, except for oxygen, whose presence will be explained later.

Other chemical elements can be classified according to their presence in two key parts of the CC tape, specifically in the buffer layers and substrate. The buffer layers on Superpower tapes include materials like lanthanum manganate (LMO), magnesium oxide (MgO), yttrium oxide (Y_2O_3), and aluminum oxide (Al_2O_3). These layers are responsible for the distribution of elements such as yttrium outside the REBCO layer, as seen in Fig.3.12c, and also explain the extended presence of oxygen throughout the examined area.

The last unanswered element is carbon, which is mainly localized on the REBCO layer, which is visible in Fig.3.12g. This carbon is likely the result of chemical reactions leading to the formation of the green coating visible in Figure 3.10.

This green coating on the REBCO layer is the non-superconducting phase YBCO Y_2BaCuO_5 (Y-211), also known as the green phase. As the concentration of the green phase increases, the superconducting pathways in the material decrease, thus reducing its overall superconducting performance.[15, 16, 17]

This phase can develop under specific conditions even in a manufactured superconductor, especially as the material ages, undergoes specific chemical changes due to environmental exposure, or when the protective layer of the superconducting layer is damaged.

In our case, it seems most likely that this YBCO phase occurred due to damage to the protective silver layer, which, after completing the demagnetization experiments, exposed the superconductor to moisture and CO_2. Aging of the tapes might have also contributed to this entire process.

Conclusion

The dissertation focused on improving the shielding properties of a magnetic cloak. The goal was to optimize the magnetic cloak's shielding by expelling the trapped magnetic field that gets captured when the cloak made from CC HTS tapes transitions into a superconducting state in an external magnetic field.

Optimization and demagnetization experiments focused on different geometries using superconducting tapes from different manufacturers. The results showed that demagnetization using SuperPower tapes was more efficient compared to Fujikura tapes. The results obtained during demagnetization showed a significant reduction in the trapped magnetic field. For the longitudinal SuperPower geometry, the field reduction was from an average trapped field of 37.575 µT to 3.0839 µT, with the best result achieved being 1.699 µT. This means that the average reduction is 91.79% and the reduction at the peak is 95.48%.

For the helical SuperPower geometry, the field reduction from the average captured field was 41.4207 µT to 1.7816 µT, with the best-achieved result being 0.142 µT. This means that the average reduction is 95.70% and the reduction at the peak is 99.66%.

In contrast, the demagnetizations of the Fujikura tapes were essentially ineffective, indicating different material properties. Importantly, magnetic field extrusion in this manner proved to be a repeatable process.

However, it was found that the demagnetization results of the cloak changed over time, likely due to gradual degradation. Therefore, susceptibility measurements were conducted alongside the demagnetization experiment.

Measuring susceptibility was suitable for simply verifying the functionality of the cloaks, as reference data measured during the production of the cloaks were available, allowing for comparison with the current data.

This degradation affected the shielding properties and the balance of superconducting and ferromagnetic parts. As the number of measurements increased, the shielding efficiency of the cloak decreased. In both geometries, the results indicated that the current cloaks have worse

properties than those with two layers of superconducting tape from 2017.

To further investigate the extent and cause of the superconducting part's damage, it was necessary to disassemble one of the cloaks, with the longitudinal geometry chosen since the tapes on it were already divided into 14.5 cm long segments.

To perform a deeper structural inspection, three different measurements were conducted transport measurement of a current , magnetic field mapping, SEM and EDX.

Transport measurements revealed that the tapes did not carry the critical current as declared by the manufacturer. These tapes showed significantly lower critical current, indicating substantial degradation. In the first (outer) layer, tapes exhibited an average 50% decrease in critical current compared to the manufacturer's value, while in all other layers, it was more than 90%.

Magnetic mapping with a Hall sensor provided visual information on the distribution of the magnetic field on the tape surfaces, showing reduced magnetic flux density in damaged areas.

Optical inspection using scanning electron microscopy and energy-dispersive X-ray spectroscopy provided detailed views of the microstructure and chemical composition of the tapes. The results of these experiments revealed significant damage to the REBCO layer on the tapes and chemical processes that resulted in carbon settling on the damaged parts.

These experiments suggest that the superconducting part of the shield was exposed to external forces, possibly trapped moisture or microvibrations during measurements, which damaged the thin silver layer of the superconducting tapes. As a result, the REBCO layer was exposed to moisture and potentially CO_2, reducing the oxygen concentration in this layer, leading to decomposition into the non-superconducting Y_2BaCuO_5 phase. [**?**] The reduced performance of individual tapes was attributed to defects visible in magnetic mapping and higher concentrations of Y_2BaCuO_5.[15, 16, 17]

In summary, this dissertation has two main contributions.

The first contribution is the developed method for demagnetizing a magnetic cloak, which allows for the expulsion of external/Earth's magnetic field that gets trapped in the cloak made of high-temperature superconductors due to the cooling of the superconducting part in an external field.

The second contribution lies in the partial investigation of the degradation of CC tapes, from which the superconducting part of the cloak was made. These tapes are widely used for power applications, such as cables, where degradation is undesirable. The extent and consequences of the degradation were examined, but the cause could not be determined, as it would require additional experiments specifically focused on this issue.
These findings are crucial for optimizing manufacturing processes and extending the lifespan of high-temperature superconducting materials used in magnetic shields.

List of Publications

Publications in CC database:

1. Solovyov,M., Šouc,J. ,**Kucharovič, M.** and Gömöry, F. "Design of Magnetic Cloak for an Alternating Magnetic Field With Multilayer ReBCO Insert," in IEEE Transactions on Applied Superconductivity, vol. 31, no. 5, pp. 1-5, Aug. 2021, Art no. 4901205, doi: 10.1109/TASC.2021.3067065.

2. **Kucharovič, M.**, Gömöry, F. and Solovyov, M., "Demagnetizing the Superconducting Part of the Magnetic Cloak," in IEEE Transactions on Applied Superconductivity, vol. 34, no. 3, pp. 1-4, May 2024, Art no. 8200404, doi: 10.1109/TASC.2024.3367616.

Attendance in international conferences

Autor

1. **Kucharovič, M.**,Gömöry, F. and Solovyov, M.: "Demagnetizing the Superconducting Part of the Magnetic Cloak" In: 16th European Conference on Applied Superconductivity - EUCAS 2023. Bologna, Poster.

Co-Autor

1. Solovyov, M.,Šouc,J., **Kucharovič,M.** and Gömöry.F,"Design of magnetic cloak for alternating magnetic field with multilayer ReBCO insert" In: The Applied Superconductivity Conference (ASC) 2021

2. Solovyov, M., **Kucharovič, M.**, Pardo, E., and Gömöry, F.: "Demagnetizing of magnetic cloak by use of dynamic magnetoresistance" In: 15th European Conference on Applied Superconductivity - EUCAS 2021. Moskva, virtual.

Citations: 2 (+ 1 autocitations)

- Solovyov,M., Šouc,J. ,**Kucharovič, M.** and Gömöry, F. "Design of Magnetic Cloak for an Alternating Magnetic Field With Multilayer ReBCO Insert," in IEEE Transactions on Applied Superconductivity, vol. 31, no. 5, pp. 1-5, Aug. 2021, Art no. 4901205, doi: 10.1109/TASC.2021.3067065.

    1. Brialmont, S.: Superconductor Science and Technology (2023) 054004
    2. Rotheudt, N.: Superconductor Science and Technology (2024) 065008

Bibliography

[1] M. Solovyov, J. Šouc, J. Kováč, F. Gömöry, E. Mikulášová, M. Ušáková, and E. Ušák, "Design of magnetic cloak for experiments in ac regime," *IEEE Transactions on Applied Superconductivity*, vol. 26, no. 3, pp. 1–6, 2016.

[2] F. Gömöry, M. Solovyov, J. Šouc, C. Navau, J. Prat-Camps, and A. Sanchez, "Experimental realization of a magnetic cloak," *Science*, vol. 335, no. 6075, pp. 1466–1468, 2012.

[3] M. Kucharovič, *Návrh a vyhotovenie supravodivej časti magnetického plášťa neviditeľnosti*. Phd thesis, Faculty of Electrical Engineering and Information Technology of STU in Bratislava, Bratislava, SK, 2018. Available at https://opac.crzp.sk/?fn=detailBiblioFormChildYGKCH&sid=6AA8E1A8284D263B469F4920F398&seo=CRZP-detail-kniha.

[4] F. Gömöry, M. Solovyov, and J. Šouc, "Layered superconductor/ferromagnet structures for magnetic field cloaking," *MRS Proceedings*, vol. 1684, p. 28–38, 2014.

[5] M. Solovyov, J. Šouc, M. Kucharovič, and F. Gömöry, "Design of magnetic cloak for an alternating magnetic field with multilayer rebco insert," *IEEE Transactions on Applied Superconductivity*, vol. 31, no. 5, pp. 1–5, 2021.

[6] M. Kucharovič, F. Gömöry, and M. Solovyov, "Demagnetizing the superconducting part of the magnetic cloak," *IEEE Transactions on Applied Superconductivity*, vol. 34, no. 3, pp. 1–4, 2024.

[7] M. Solovyov, J. Šouc, F. Gömöry, M. O. Rikel, E. Mikulášová, M. Ušáková, and E. Ušák, "Bulk and cc-tape based superconducting shields for magnetic cloaks," *IEEE Transactions on Applied Superconductivity*, vol. 27, no. 4, pp. 1–4, 2017.

[8] J. Souc, M. Solovyov, F. Gömöry, J. Prat-Camps, C. Navau, and A. Sanchez, "A quasistatic magnetic cloak," *New Journal of Physics*, vol. 15, p. 053019, may 2013.

[9] M. Godár, *Voltampérové charakteristiky supravodivých pások s lokálnym znížením kritického prúdu*. Diploma thesis, Faculty of Electrical Engineering and Information

Technology of STU in Bratislava, Bratislava, SK, 2023. Available at https://opac.crzp.sk/?fn=docview2ChildQ14O7F&record=30EAE6FD1E2AFEEA10C7A01C8F40&seo=CRZP-Prehliadanie-prÃąc.

[10] M. Soloviov, *AC losses in coated conductors*. Phd thesis, Faculty of Electrical Engineering and Information Technology of STU in Bratislava, Bratislava, SK, 2011.

[11] J. Kvítkovič and M. Polák, "Cryogenic microsize hall sensors," *EUCAS 93. - Applied Superconductivity 1.*, vol. 1, p. 1625, 1993.

[12] "Scanning Electron Microscopy | Nanoscience Instruments — nanoscience.com." https://www.nanoscience.com/techniques/scanning-electron-microscopy/. [Accessed 08-05-2024].

[13] C. Temiz, "Scanning electron microscopy," in *Electron Microscopy* (M. Mhadhbi, ed.), ch. 1, Rijeka: IntechOpen, 2022.

[14] "Scanning electron microscope (SEM) | Definition, Images, Uses, Advantages, & Facts — britannica.com." https://www.britannica.com/technology/scanning-electron-microscope. [Accessed 08-05-2024].

[15] M. Rotta, D. K. Namburi, Y. Shi, A. L. Pessoa, C. L. Carvalho, J. H. Durrell, D. A. Cardwell, and R. Zadorosny, "Synthesis of y_2bacuo_5 nano-whiskers by a solution blow spinning technique and their successful introduction into single-grain, ybco bulk superconductors," *Ceramics International*, vol. 45, no. 3, pp. 3948–3953, 2019.

[16] Y. Slimani, E. Hannachi, A. Koblischka-Veneva, and M. R. Koblischka, "Excess conductivity analysis of an ybco foam strut and its microstructure," *Materials (Basel)*, vol. 17, p. 1649, Apr 2024.

[17] "Discovery of superconductivity at 93 k in ybco: The view from ground zero." https://ethw.org/First-Hand:Discovery_of_Superconductivity_at_93_K_in_YBCO:_The_View_from_Ground_Zero. [Accessed 30-05-2024].